Study of the crystallization of leucite in feldspar glass matrix

M. D. Fonseca · F. T. Silva · T. Ogasawara

Abstract Feldspathic glass–ceramics reinforced with leucite are usually used in dental prosthesis. This study focused on leucite crystallization kinetics due to its importance to the end product of a dental crown processing. Leucite grains were nucleated and grown from feldspathic glass frit powders with particle size smaller than 45 μm. The nucleation and crystallization kinetics of leucite crystals in the glass matrix was investigated under isothermal and non-isothermal conditions through differential thermal analysis. The samples were also characterized by X-ray diffraction and scanning electron microscopy. The temperature of maximum nucleation rate was determined from the DTA curves of samples heat treated at different temperatures. The activation energy (E) of leucite crystallization was determined by the Kissinger method and the Avrami parameter (n) indicated that surface crystallization is the dominant mechanism in the glass.

Keywords Glass–ceramics · Leucite nucleation · Leucite crystallization · Differential thermal analysis

Introduction

Glass–ceramics are polycrystalline materials usually produced by melting, solidification, and controlled crystallization of a glass. They have several relevant properties: high hardness, abrasion resistance, thermal shock resistance, high chemical stability and low thermal and electrical conductivities. Nowadays glass–ceramics are an attractive option for dental restorations, providing optical properties similar to those of natural teeth.

The transformation of glass into glass–ceramics occurs through an appropriate heat treatment where crystals are nucleated and grown in a glass matrix possessing outstanding properties and applicability [1, 2]. In this regard, several studies of crystallization have been performed using data of thermal analysis, as DTA obtained through isothermal and non-isothermal methods [3].

A high quality glass–ceramic requires a microstructure made up of small grains homogeneously dispersed in the glass matrix, a feature found in many silicate systems when they are subjected to a controlled cooling rate [2, 4].

Leucite ($K_2O \cdot Al_2O_3 \cdot 4SiO_2$), a potassium aluminum-silicate mineral, has been commonly used as a reinforcing phase in feldspathic porcelains for dental prosthesis. This mineral has a high coefficient of thermal expansion (CTE) exhibiting a polymorphic phase transformation from cubic to tetragonal. The significant thermal expansion that exists between the tetragonal leucite crystals ($22.3–25 \times 10^{-6}$ °C^{-1}) and the glass matrix (8.6×10^{-6} °C^{-1}) provides tangential compressive stresses around the crystals, which are responsible for its increased toughness [5] and machinability [6]. From Cattell et al. [5], the volumetric fraction of tetragonal leucite in dental porcelains varies in the range 17–45%.

This study aimed at determining the temperature of maximum nucleation rate and the kinetic parameters of leucite crystallization.

M. D. Fonseca (✉) · F. T. Silva · T. Ogasawara
Department of Metallurgical and Materials Engineering, UFRJ/ COPPE-PEMM—Federal University of Rio de Janeiro, Alberto Luiz Coimbra Institute of Graduate Course and Research of Engineering, Av. Horácio Macedo, 2030—CT/UFRJ—Bloco F sala F210—Ilha do Fundão, Caixa Postal 68505, Rio de Janeiro, RJ 21941-972, Brazil
e-mail: mdfonseca@metalmat.ufrj.br

Experimental

Leucite grains were nucleated and grown from feldspathic glass frit powders which were produced by melting a mixture composed by (in wt%) 77.82% Brazilian Armil feldspar, 2.62% Al_2O_3, 7.77% Na_2O_3, 8.65% K_2CO_3, 2.49% borax, and 0.64% CeO_2. The chemical composition of the Armil feldspar was (in wt%) 66.0% SiO_2, 20.0% Al_2O_3, 5.5% K_2O, 5.9% Na_2O, 0.26% CaO, 0.34% P_2O_5, 0.07% Rb_2O, and 0.11% NiO. The melting of this mixture was carried out in a muffle furnace at 1200 °C for 3 h inside an alumina crucible, followed by iced-water quenching and grinding to achieve particle size below 45 μm.

Samples of glass frit (9 mg in an alumina pan) were submitted to heat treatments in an apparatus of differential thermal analysis (Shimadzu DTA-50) under air flow. In the case of isothermal treatment the heating rate was 10 °C min^{-1} with a dwell time of 30 min in the nucleation temperatures (200, 250, 300, 350, and 400 °C) followed by heating up to 1100 °C at the same heating rate. In non-isothermal treatment four different heating rates ($\beta = 2.5, 5.0, 10,$ and 20 °C min^{-1}) were used to reach temperatures up to 1100 °C.

The resulting sinters were submitted to XRD (Shimadzu XRD-6000), using CuKα radiation (30 kV, 30 mA), the 2θ range was 5–80°. SEM images were obtained by using a Jeol 6460 LV microscope operated at 20 kV with the samples previously coated with gold in an Emitch K550 sputtering unit.
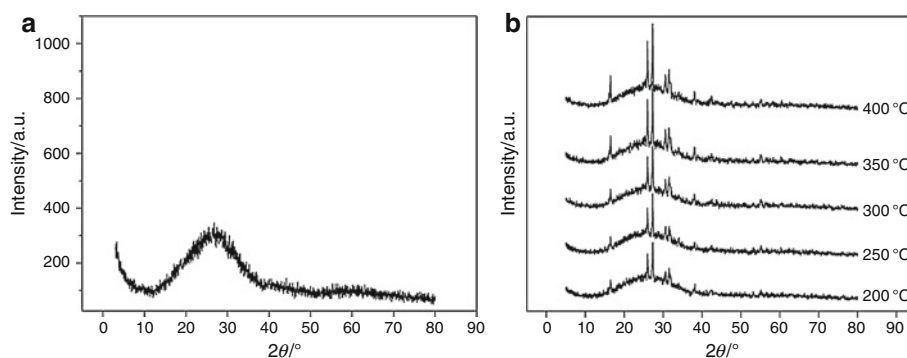
The morphology of leucite crystals was characterized by SEM, after polishing with alumina and further etching with 0.1% fluoridric acid aqueous solution for 50 s followed by water rinsing. Representative SEM micrographs were analyzed by quantitative ceramography using an image analysis software (Image-Pro Plus 4.0).

Results and discussion

Determination of the maximum nucleation rate

Figure 1a shows the X-ray diffraction pattern of the glass frit powder, confirming its amorphous nature. Figure 1b shows the X-ray diffraction of the same frit after heat treatment for the nucleation of leucite at different temperatures followed by its crystallization up to 1100 °C at the same heating rate. Heating the samples up to 1100 °C is usually the thermal treatment employed to get the desired densification of the glass powder compact, so it provides due to information about the microstructure of the glass–ceramics under practical processing conditions.

The experimental method used to determine the maximum nucleation rate from the glass phase was that suggested by Ray and Day [7], the height of the crystallization peak achieved from DTA (δT)p, being proportional to the nuclei concentration in the glass matrix. Figure 2 shows the height of crystallization peak for different nucleation temperatures. The maximum nucleation rate of the glass was obtained around 250 °C.

It is well-known that high content of leucite crystals inside the glass matrix improves the mechanical properties of glass–ceramics [8]; so it is interesting to define the temperature for the maximum nucleation rate for a glass–ceramic possessing the desired microstructure as a result of controlled nucleation and crystallization of leucite. If volumetric nucleation dominates, the temperature of the maximum nucleation is equal to or higher than the glass transition temperature. If surface nucleation takes place, the temperature for the maximum nucleation rate is lower than the glass transition temperature [9], as observed in this study.

Figure 3 shows the SEM microstructure of the glass frit after heat treatment of nucleation of leucite crystals at 250 °C followed by heating to 1100 °C. It can be observed that the leucite crystals are fairly homogeneous and relatively well-dispersed in the glass matrix. The mean particle size and volume fraction of leucite crystals for different nucleation temperatures were determined by ceramography, as shown in Table 1.

Determination of the kinetic parameters of leucite crystallization under non-isothermal conditions

Figure 4 shows crystallization peaks of leucite recorded from the DTA curve at different heating rates as a function
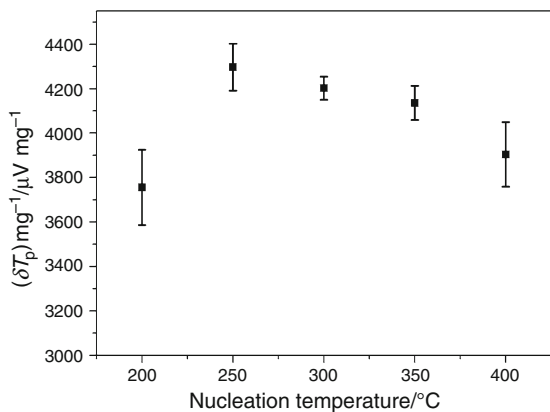
Fig. 1 X-ray diffraction of the glass frit **a** confirming its amorphous nature and **b** nucleated at different temperatures and further heated at 1100 °C at the same heating rate

Fig. 2 Height of the crystallization peak for different nucleation temperatures with dwell time of 30 min
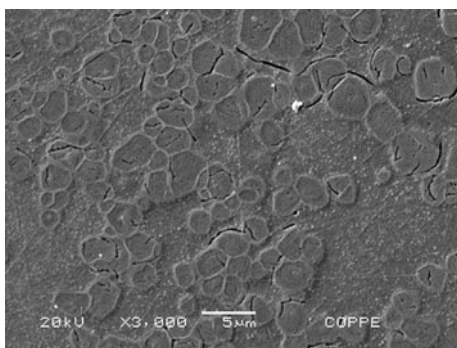

Fig. 3 SEM image of leucite crystals

Table 1 Mean particle size and volume fraction of leucite crystals at different nucleation temperatures followed by heating to 1100 °C

Nucleation temperature/ °C	Mean particle size/μm	Volume fraction/%
200	2.2 ± 0.7	25.4 ± 0.2
250	2.1 ± 0.7	34.5 ± 0.2
300	2.4 ± 0.7	29.4 ± 0.5
350	2.4 ± 0.8	29.2 ± 0.3
400	2.5 ± 0.7	28.4 ± 0.5

of temperature. Those graphs were normalized in order to obtain a better definition of the crystallization peak temperatures and the width of the crystallization peak at half maximum. Table 2 shows the peak temperatures for the different heating rates. Those peaks were used to calculate the activation energy of leucite crystallization by the Kissinger equation [10–15]:

$$\ln\left(\frac{\beta}{T_p^2}\right) = -\frac{E}{RT_p} + C \qquad (1)$$

where β is the heating rate, E is the activation energy, R is the gas constant, T_p is the exothermic peak temperature, and C is
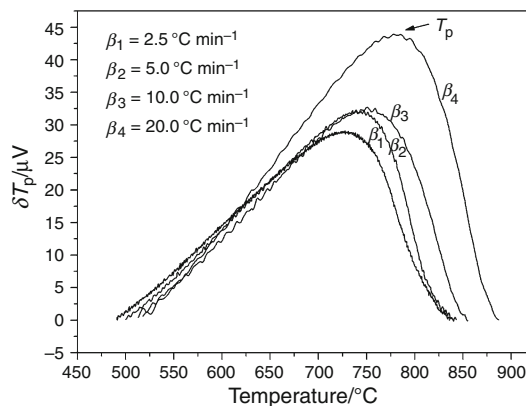

Fig. 4 Normalized DTA curves for different heating rates

Table 2 Peak temperatures of the normalized DTA curves for the different heating rates

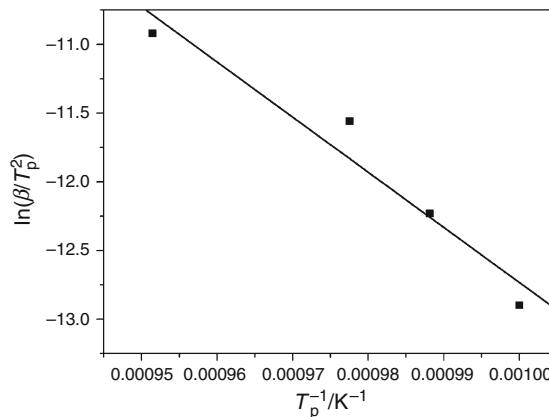| β/°C min^{-1}	T_p/°C
2.5	727
5.0	739
10	750
20	778

Fig. 5 Kissinger plot from the normalized DTA curves. The slope is the activation energy of the process

a constant. The activation energy ($E = 333 \pm 57$ kJ mol^{-1}) was determined from the slope of the plot of $\ln(\beta/T_p)$ vs. $1/T_p$ shown in Fig. 5. The magnitude of the activation energies obtained in this study is in agreement with those reported in literature [4, 16].

Figure 6 shows the microstructure of the glass frit heat treated at 10 °C min^{-1} up to 1100 °C, where the fairly rounded homogeneous leucite crystals are well-dispersed in the glass phase. The mean particle size of leucite crystals and its volume fraction were, respectively, (2.0 ± 0.7) μm and (20.7 ± 0.2)%.

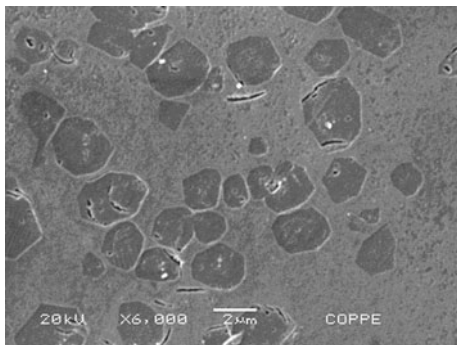**Fig. 6** SEM image of leucite crystals heat treated at rate of 10 °C min^{-1} up to 1100 °C

The Avrami parameter (n), related to the dominant crystallization mechanism, was determined by using the following equation [7, 10, 17, 18]:

$$n = \frac{2.5}{\Delta T} \cdot \frac{T_p^2}{(E/R)} \qquad (2)$$

where T_p is the exothermic peak temperature, ΔT is the width of the crystallization peak at half maximum, E is the activation energy, and R is the gas constant. The Avrami parameter (n) near 1 indicates surface crystallization while near 3 denotes volumetric crystallization [7]. In this study, the Avrami parameter was equal to 0.4 indicating that the surface crystallization of leucite is dominant mechanism. The parameter n obtained in this study was similar to that obtained by Tosic et al. [4, 16] for particle size of the glass frit between 38 and 45 μm.

Conclusions

X-ray diffraction patterns confirmed that the feldspathic glass powder prepared by quenching its melt inside iced-water is effectively an amorphous material. It was also evidenced that leucite was the only crystalline phase present in the glass matrix after crystallization heat-treatment.

The temperature of maximum nucleation rate of leucite crystals was around 250 °C.

The volume fraction of leucite crystals remained in the range between 17 and 45%, which is an indication that the glass–ceramic is suitable for dental ceramics application.

The activation energy of leucite crystallization was (333 ± 57) kJ mol^{-1}, similar to other leucite glasses reported in the literature. The Avrami Parameter ($n = 0.4$) indicated that surface crystallization is the dominant mechanism in the glass matrix.

References

1. Gorman CM, Hill RG. Heat-pressed ionomer glass-ceramics. Part I: an investigation of flow and microestrure. Dent Mater. 2003;19: 320–6.
2. Cabral AA, Fokin VM, Zanotto ED, Chinaglia CR. Nanocrys-tallization of fresnoite glass. I. Nucleation and growth kinetics. J Non-Cryst Solids. 2003;330:174–86.
3. Cheng K. Determining crystallization kinetic parameters of Li$_2$O–Al$_2$O$_3$–SiO$_2$ glass from derivative differential thermal analysis curves. Mater Sci Eng B. 1999;60:194–9.
4. Tosic MB, Dimitrijevic RZ, Mitrovic MM. Crystallization of leucite as the main phase in glass doped with fluorine anions. J Mater Sci. 2002;37:2293–303.
5. Cattell MJ, Chadwick TC, Knowles JC, Clarke RL. The crys-tallization of an aluminosilicate glass in the K$_2$O–Al$_2$O$_3$–SiO$_2$ system. Dent Mater. 2005;21:811–22.
6. Song X-F, Yin L, Han Y-G. In-process assessment of dental cutting of a leucite-reinforced glass-ceramic. Med Eng and Phys. 2009;31:214–20.
7. Ray CS, Day DE. Determining the nucleation rate curve for lithium disilicate glass by differential thermal analysis. J Amer Ceram Soc. 1990;73:439–42.
8. Souza JCM, Nascimento RM, Martinelli AE. Efeito da conden-sação e queima na formação de defeitos microestruturais em cerâmicas feldspáticas dentárias. Cerâmica. 2007;53:288–94.
9. Zanotto ED. Isothermal and adiabatic nucleation in glass. J Non-Cryst Solids. 1987;89:361–70.
10. Zhang Y, Lv M, Chen D, Wu JQ. Leucite crystallization kinetics with kalsilite as a transition phase. Mater Lett. 2007;61:2978–81.
11. Takei T, Kameshima Y, Yasumori A, Okada K. Crystallization kinetics of mullite from Al$_2$O$_3$–SiO$_2$ glasses under non-isother-mal conditions. J Eur Ceram Soc. 2001;21:2487–93.
12. Park HC, Lee SH, Ryu BK, Son MM, Lee HS, Yasui I. Nucle-ation and crystallization kinetics of CaO–Al$_2$O$_3$–2SiO$_2$ in pow-dered anorthite glass. J Mater Sci. 1996;31:4249–53.
13. Araújo EB, Idalgo E. Non-isothermal studies on crystallization kinetics of tellurite 20Li$_2$O–80TeO$_2$ glass. J Therm Anal Calo-rim. 2009;95:37–42.
14. Majhi K, Varma KBR. Crystallization kinetics of SrBi$_2$B$_2$O$_7$ glasses by non-isothermal methods. J Therm Anal Calorim. 2009; 98:731–6.
15. Gupta N, Dalvi A. Thermal stability and crystallization kinetics in superionic glasses using electrical conductivity-temperature cycles. J Therm Anal Calorim. 2010;102:851–5.
16. Tosic MB, Mitrovic MM, Dimitrijevic RZ. Crystallization of leucite as the main phase in aluminosilicate glass with low fluorine content. J Mater Sci. 2000;35:3659–67.
17. Augis JK, Bennet JE. Calculation of the Avrami parameters for heterogeneous solids state reactions using a modification of the Kissinger method. J Therm Anal Calorim. 1978;13:283–92.
18. Li Y, Liang K, Xu B, Cao JW. Crystallization mechanism and microstructure evolution of Li$_2$O–Al$_2$O$_3$–SiO$_2$ glass-ceramics with Ta$_2$O$_5$ as nucleating agent. J Therm Anal Calorim. 2010;101:941–8.